

## Evaluation of an IQ demodulator

J. Zhang

Microwave group, IHEP, China

T. Matsumoto and T. Higo

Accelerator Laboratory, KEK, Japan

### Abstract

We evaluated an IQ demodulator aiming at the usage for the phase measurement of the reflected pulse from the accelerator structure test at Nextef. The characterization of the IQ demodulator was made by varying the input power level both for LO and RF input. We conclude that this device can be used for the identification of the reflected phase different by  $\pm 120$  degrees depending on which cell the breakdown happens. The further evaluation of the device was tried with fitting the output (I, Q) in the complex plane but could not get an practical solution to calibrate the module over a dynamic range of 20dB.

## Motivation

In KEK, high gradient tests on accelerator structures are ongoing at Nexter<sup>[1]</sup>. We want to identify the position of the breakdown in the accelerator structure. Until now, KEK uses only the crystal signals of forward, reflected and transmitted power to estimate the position and timing of the breakdown. Since the signals are noisy, it is not straightforward to identify the position by using such simple information clearly. If we add the information of the reflected phase, we may get a better identification of the position<sup>[2]</sup>, because the reflection from a certain cell differs in phase by 240 degrees from that of the next cell.

Since the reflected power changes a lot depending on the breakdown event, such device as double balanced mixer cannot easily be used without tedious calibration over a large dynamic range. This is the motivation to apply an IQ demodulator for the evaluation of the phase in a large dynamic range in its input power. Figure 1 shows the schematic of the phase measurement by using an IQ demodulator. We use the forward wave from the directional coupler connected to LO input, while the backward wave to the RF input.

Figure 2 shows the reflection phase related to the breakdown position. In this paper, we define the phase  $\phi$  as follows, where  $k$  is the wave number in the waveguide and  $z$  the length along the waveguide,

$$e^{j\phi} = e^{j(\omega t - k z)}$$

and this complex number can simply be shown in real-imaginary, complex plane. If the first breakdown occurs at the 1st cell, the second one may occur at cell 2nd or 3rd. If the second breakdown after the first one came from the cell 2nd, the phase change from forward and backward wave of the first breakdown and the second one will give a 240deg phase delay, and that at the 3rd cell will give a 480deg phase delay. Figure 2 also shows an example of the first breakdown happens in 0deg. In other words, the phase difference of the forward wave and backward wave equal to 0deg. Also the output of IQ demodulator equal to 0deg. The second B.D. in place 2nd cell will locate at 120deg, in 3rd cell will locate at 240deg. Here we want to identify which cell the second breakdown comes from in a large dynamic range of input power.

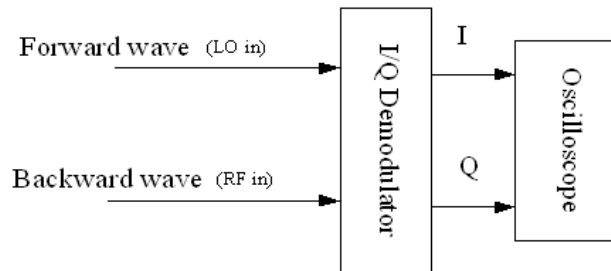


Fig. 1 The schematic of measurement of reflection phase using IQ demodulator.

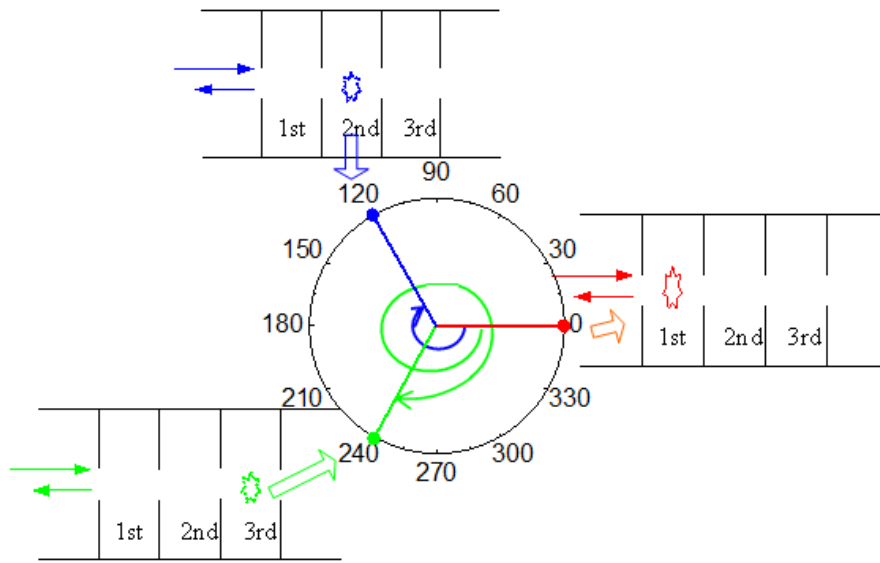


Fig. 2 The reflection phase related to the cell of the breakdown.

## Specifications of the IQ demodulator

We bought the same IQ demodulator,<sup>[3]</sup> which SLAC NLCTA is using for the same purpose. A picture is shown in Fig. 3. The typical specification is shown below.

- ✧ P/N: IDH-02-458 0843 (Pulsar microwave)
- ✧ Carrier (LO) frequency: 10-12GHz
- ✧ RF frequency:  $LO \pm 100\text{MHz}$
- ✧ Phase balance: 10 Deg
- ✧ Operating LO power level:  $+10 \pm 0.5\text{dBm}$
- ✧ Operating RF power level:  $-10 \pm 0.5\text{dBm}$
- ✧ Max. LO power level:  $+20\text{dBm}$
- ✧ Max. RF power level : $+13\text{dBm}$



Fig. 3 Picture of the IQ demodulator.

## Characterization of the IQ demodulator

Figure 4 shows the measurement setup. Firstly, the phase shifter and the attenuators were calibrated by using network analyzer. Figure 5 is the phase shifter close-up view. Figure 6 shows the result of the calibration of the phase shifter at 11.424GHz. The indication of the phase shifter was used as the x-axis.

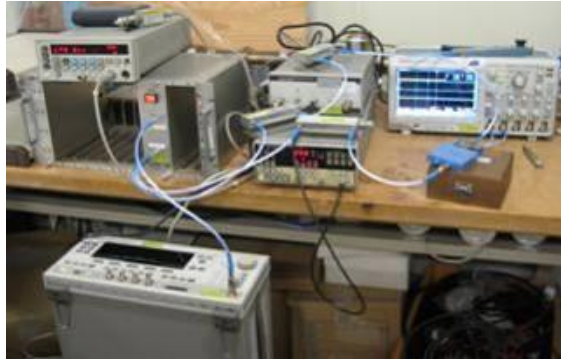


Fig. 4 Whole setup with SG, amplifier, IQ, pulse modulator, etc.

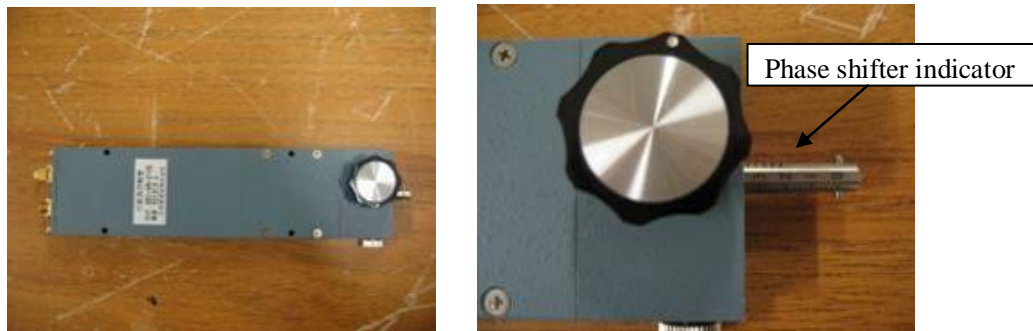


Fig. 5 Phase shifter close-up view.

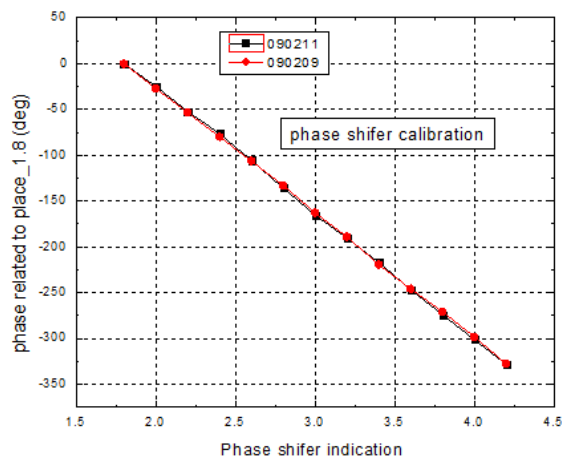


Fig. 6 The phase shifter calibration.

The output phase, defined as  $\text{Arctan}(Q/I)$ , was then measured as function of input phase difference of LO in and RF in. In Table 1 are listed all the combinations of input powers at LO in port and RF in port. Figure 7 is the measured output phase versus the input phase for different input power combinations. Figure 8 is the deviation of the output phase to the input phase. The

value is within -15 to +45 degrees, which is well less than half of 120 degrees. This means that this device can be used for the phase difference by some multiple of 120 degrees. This situation can be explained more in detail in Figure 9.

Table 1 The input power combination

P_LO (dBm)	20	20	20	10	10	10	0	0	0
P_RF (dBm)	10	0	-10	10	0	-10	10	0	-10

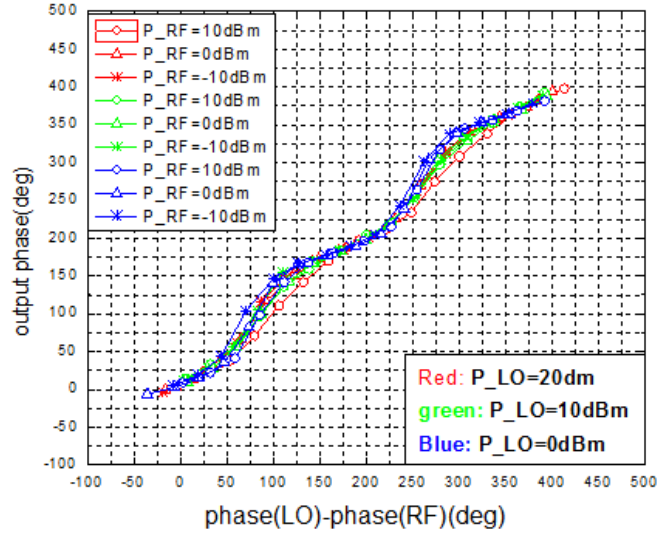


Fig. 7 Measured phase vs. input phase difference

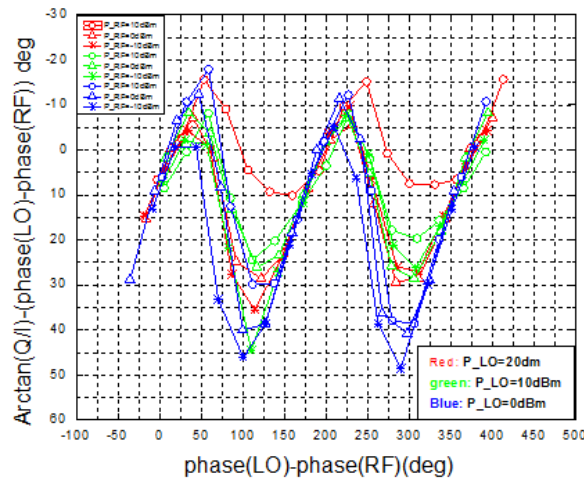


Fig. 8 Output phase difference versus input phase of the IQ device

Figure 9 was made from the data of figure 7. The horizontal axis is the input phase difference between the RF in and the LO in of the IQ demodulator. The vertical axis is the output phase of IQ, equal to  $\arctan(Q/I)$ . The error bars show the output phase range for different power combinations. Let us consider an example case as shown in Figure 9. If the breakdown at the 1st cell makes the input phase difference equals to 180 degrees, the IQ output will be located at the brown circle (a). Then, the breakdown at the next cell will make the input phase difference equals to  $180+120=300$  degrees, resulting in the IQ output located at the red circle (b). The breakdown at the next cell in opposite direction from the previous one will make the input phase difference equals to  $180-120=60$  degrees, resulting in the IQ output located at the green circle (c). If we move the

circle (b) to (b') and (c) to (c') for checking the separation with each other, we can clearly see that no overlap exist.

From this consideration, we conclude that this IQ demodulator can be used to identify the breakdowns at the cells, which create the reflection phases with difference by  $\pm 120$  degrees.

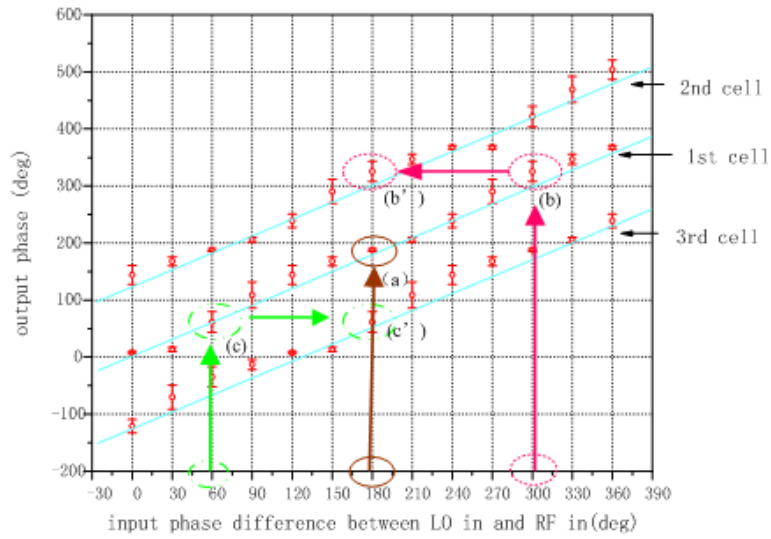


Fig. 9 Output phase versus input phase with curves at  $+120$  or  $-120$  degrees to show the case with different reflection phase from the nominal one at the center curve.

## Trial for the detailed characterization of the device

During the above measurements, we noticed that there was a fairly big error in sinusoidal variation in 180 degree interval, as shown in Fig. 8. We understand that the contour shape of the output (I, Q) points deforms as characterized by several parameters<sup>[4]</sup>, gain of each channel, skew angle and DC offset. We tried to understand the mechanism of the error and did a fitting of the raw data using the ellipse shape in a complex (I, Q) plane. Figure 10 shows an example of the fitting at the nominal power level chosen by the maker, the LO input power of 10dBm and the RF in input power of -10dBm. In the figure, blue asterisks are the initial measured data, the red curve is the ellipse fitting and the green circles are the corrected data points calibrated by the fitted parameters. Table 2 shows the value of the correction parameters. In the table, “a” is the value of the major axis, “b” of the minor axis, “phi” the angle between the x-axis and the major axis in degrees, x0\_in is the center at the x axis of the tilted ellipse, y0\_in that at the y axis of the same ellipse.

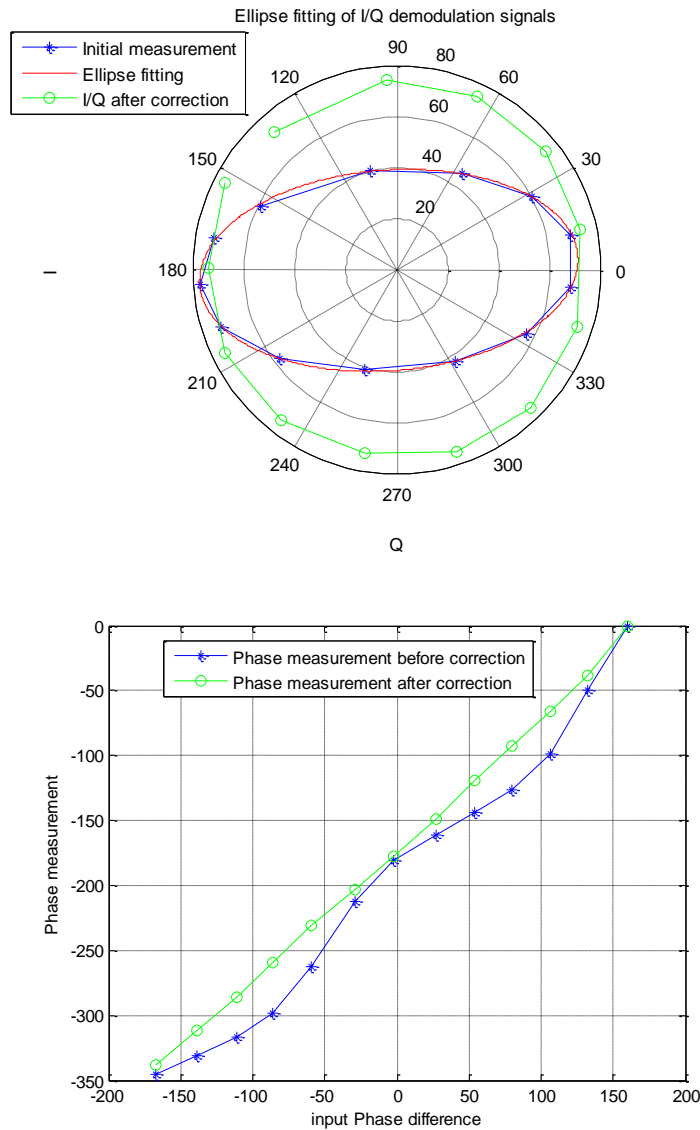


Fig. 10 (I, Q) diagram for the case with a recommended power combination.

Table 2 Correction parameters. The column in red letters is the recommended one by the company.

P_LO (dBm)	20	20	20	10	10	10	0	0	0
P_RF (dBm)	10	0	-10	10	0	-10	10	0	-10
a	396	194	64	346	206	74	243	226	79
b	308	106	34	286	113	39	123	87	32
phi	-34	-5	-3	-16	-6	-4	0	-2	0
x0_in	3.2	1.9	-4.4	5.8	2.3	-3.2	9.3	4.3	-2.5
y0_in	-4.7	-0.87	-0.4	0.2	-0.6	-0.17	7.5	0.43	0.15
A	1.02	1	1	1.03	1	1.02	1.01	1.01	1.01
B	-34.8	8.48	25.5	-6.57	6.24	9.57	13.2	13.4	20

The correction can be described as bellow:

$$\begin{bmatrix} I_{ellicor} \\ Q_{ellicor} \end{bmatrix} = \begin{bmatrix} \cos(\phi) & \sin(\phi) \\ -\sin(\phi) & \cos(\phi) \end{bmatrix} \begin{bmatrix} 1 & 0 \\ 0 & \frac{a}{b} \end{bmatrix} \left( \begin{bmatrix} I \\ Q \end{bmatrix}_{meas} - \begin{bmatrix} x0\_in \\ y0\_in \end{bmatrix} \right)$$

Figure 11 is the input phase and the output phase after ellipse correction. Figure 12 is the deviation of the output phase to the input phase. Figure 11 shows that the output is more linear than the raw data.

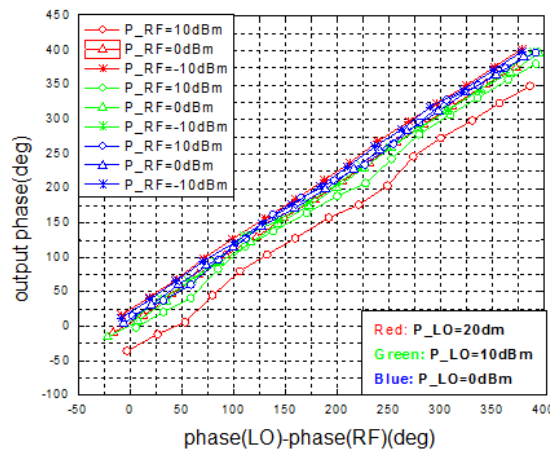


Fig. 11 The input phase and output phase relationship after correction

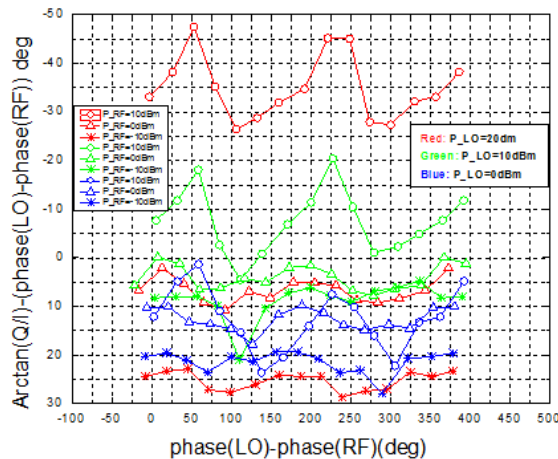


Fig. 12 Output phase difference versus input phase after ellipse correction

After the ellipse correction, we made a linear fitting of the graph in figure 11. Figure 13 is an example of the fitting at the nominal power. Then we get the slope A and the interception B. After this linear fitting, we obtain the fully corrected value as below:

$$\begin{bmatrix} I\_cor \\ Q\_cor \end{bmatrix} = \frac{1}{A} \cdot \left( \begin{bmatrix} I\_lincor \\ Q\_lincor \end{bmatrix} - B \right)$$

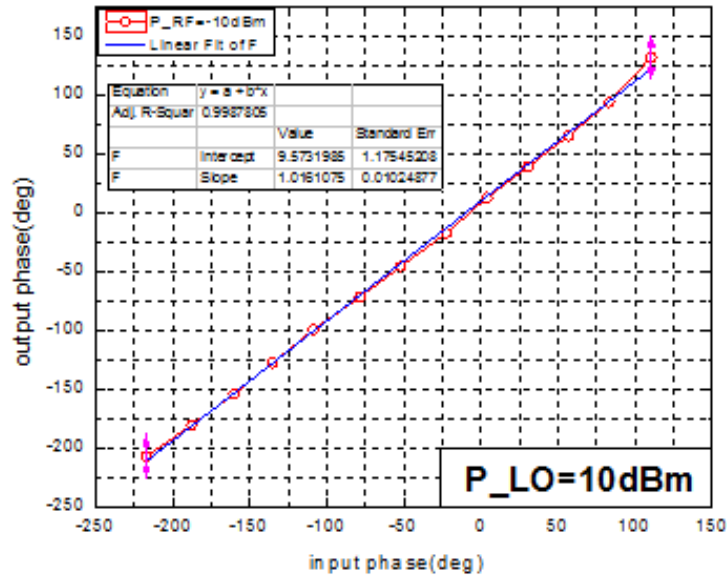


Fig. 13 Linear fitting result

Now, the output phase equals to the input phase deference of LO in and RF in. However, the fitting parameters do not follow a simple functional form as functions of RF power and LO power, we gave up to adopt the correction described in this section.

## Pulse response and band width

The pulse width we typically operate is from 50ns to 250ns. Figure 14 is the rise time measurement results when the pulse width is 250ns. A crystal detector(Agilent 8473B) is used to measure the input signal, and the signal's rise time(10-90%) is 13.3ns. The IQ demodulator output signal's rise time is 1.6ns. From this comparison, we see that the IQ is faster than the crystal detector. If we use this IQ demodulator as a device to measure the phase lasting more than 10 nsec, we conclude that it is fast enough.

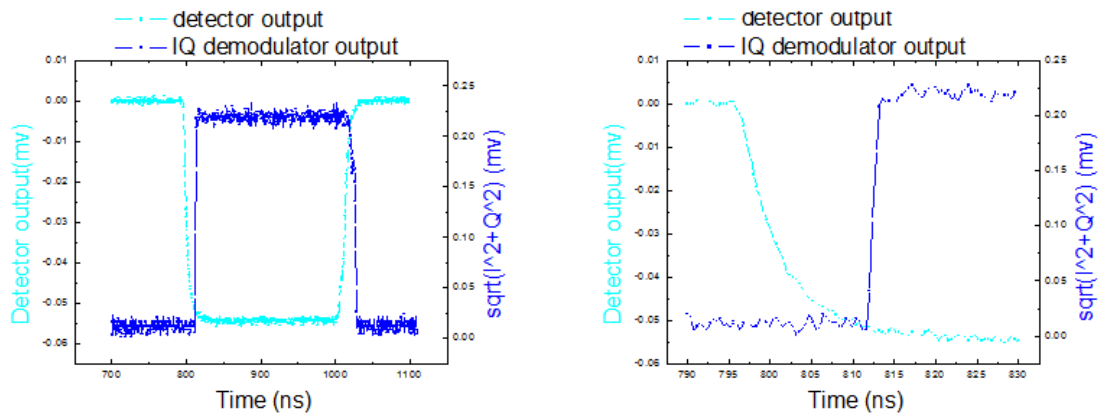


Fig. 14 Rise time measurement. One with crystal detector and the other one by IQ demodulator.

Figure 15 shows the band width of this IQ demodulator. The output power is normalized by input power. The flat part of the band width is from 8.5GHz to 13.5GHz. For the announced band width of this device from 10-12GHz, it is flat enough for our usage.

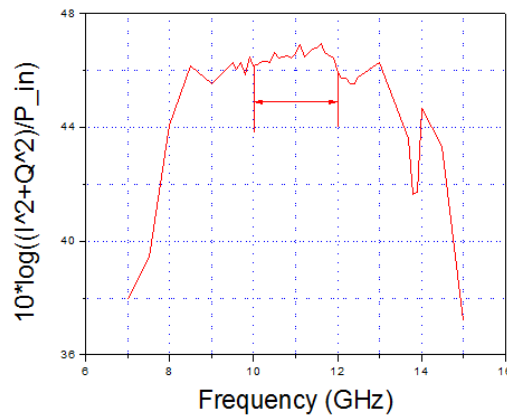


Fig. 15 Band width of the IQ demodulator.

## Conclusion

We conclude that the IQ present demodulator can be used for the identification of the reflected phase different by  $\pm 120$  degrees over the dynamic range of 20dB, meaning that we can distinguish the breakdowns at the next cell. The response of this device is fast enough to evaluate the phase information of the pulses with its width more than 10 nsec.

We will apply this device to the measurement at Nextef.

The further evaluation of the device was tried with fitting the output (I, Q) in the complex plane but could not get any smooth calibration formula over the dynamic range of 20dB. For this we may need the analysis of this device based on more physical understanding and we gave up this time.

## Acknowledgment

This study is supported by a short-term invitation program by KEK. One of the authors, Dr. Zhang Jingru, could come and stay at KEK to work for the X-band of KEK. She would like to extend her deep thanks to Dr. Toshiyasu Higo, Dr. Kazue Yokoyama, Dr. Shuji Matsumoto in KEK Accelerator Laboratory for their invitation and supporting. Dr. Toshiyasu Higo gave her many beneficial advices on the work of accelerator measurement and IQ demodulator evaluation. Dr. Geng Zheqiao in DESY also gave her valuable talks about the IQ demodulator evaluation. Dr. Toshihiro Matsumoto also made various instructive advices careful read this manuscript. She would also appreciate Ms. Emiko NISHIMURA in the KEK International Affairs Division for her helping with the visit procedure, and all the friends in China and Japan who are involved in the research visiting, both at a scientific level and at the personal affairs.

## References

- [1] S. Matsumoto, Int'l Linear Accelerator Conference, LINAC08, THP053, Vancouver, 2008.
- [2] C. Adolphsen, "X-band Structure Test at NLCTA," CLIC08 Workshop, CERN, 2008.  
<http://project-clic08-workshop.web.cern.ch/project-clic08-workshop/>
- [3] C. Adolphsen, Selection of the IQ demodulator, private communication.
- [4] T. Schilcher, "Digital Signal Processing to RF Applications," CAS, Sigtuna, Sweden, June, 2007.